The energy uncertainty could be reduced by better chemistry, such as cupferron-solvent methods, and by the use of a multichannel coincidence analyzer.

A proposed decay scheme for Sn^{113} is shown in Fig. 4.

ACKNOWLEDGMENTS

The writers wish gratefully to acknowledge the support given this research by the U. S. Atomic Energy Commission. The interest and help of numerous colleagues is appreciated. Thanks are to be expressed to Dr. H. C. Thomas, Dr. W. G. Holladay, Dr. G. J. Nijgh, Dr. E. A. Jones, and Dr. C. D. Curtis for the elimination of many errors in principle and in expression. However, those which remain are accountable to the authors. Gratitude is extended to William F. Frey for guidance on and supervision of radiation safety, and to Randall W. Carter, and Roy A. Parker for help with chemical problems.

PHYSICAL REVIEW VOLUME 119, NUMBER 4 AUGUST 15, 1960

Internal Conversion Electrons Following Coulomb Excitation of Highly Deformed Odd-A Nuclei*

E. M. BERNSTEIN† AND R. GRAETZER

Physics Department, University of Wisconsin, Madison, Wisconsin

(Received March 23, 1960)

The internal conversion electrons emitted following Coulomb excitation of Eu^{153}, Dy^{161}, Dy^{163}, Ho^{165}, Tm^{169}, Lu^{175}, and Ta^{181} have been measured. The relative intensities of the decay transitions from the first two rotational states of these isotopes have been compared with the predictions of the rotational model of Bohr and Mottelson. In general, there is good agreement between the experiment and theory; however, the results for the Dy isotopes indicate some disagreement which is outside the experimental uncertainty. For Eu^{153}, Dy^{163}, and Lu^{175} transitions involving intrinsic states were observed in addition to the rotational transitions. The reduced $E2$ transition probabilities for these intrinsic transitions are appreciably larger than single-particle estimates. The first rotational state in Lu^{176} was observed with a natural Lu target. The data indicate that this transition is predominantly $M1$.

I. INTRODUCTION

IT has been pointed out previously[1–3] that Coulomb excitation of highly deformed odd-A nuclei is an excellent method for checking the predictions of the rotational model of Bohr and Mottelson. The most accurate experiments of this type up to the present time have been the measurements[4] of the inelastically scattered particles. The inelastic scattering experiments, however, only measure the $E2$ transition probabilities between the ground state and the excited states. In order to obtain information concerning the $M1$ transition probabilities and the $E2$ transition probabilities between the excited states, one must measure the decay radiations—gamma rays or internal conversion electrons.

The advantages and disadvantages associated with measuring the internal conversion electrons rather than the gamma rays have been discussed in detail elsewhere.[1–3] In principle the same information can be obtained from the observation of the gamma rays or the internal conversion electrons; however, at the present time a more complete and more accurate check of the model can be obtained from the internal conversion measurements.

In the present experiment the internal conversion electron spectra emitted following Coulomb excitation of Eu^{153}, Dy^{161}, Dy^{163}, Ho^{165}, Tm^{169}, Lu^{175}, and Ta^{181} have been measured. With electric quadrupole excitation of these odd-A nuclei one excites the first two rotational states above the ground state. There are, therefore, three transitions from the decay of these states: the transition from the first rotational state to the ground state, the cascade transition from the second rotational state to the first, and the crossover transition from the second rotational state to the ground state.

The basic techniques used in the present experiment are essentially the same as those used in previous experiments.[2,3,5,6] However, these techniques have been greatly improved with the result that the experimental uncertainties have been significantly reduced. Also, in the earlier experiments the weak conversion lines of

* Work supported by the U. S. Atomic Energy Commission, and by the Graduate School from funds supplied by the Wisconsin Alumni Research Foundation.

† Present address: Institute for Theoretical Physics, Copenhagen, Denmark.

[1] K. Alder, A. Bohr, T. Huus, B. Mottelson, and A. Winther, Revs. Modern Phys. **28**, 432 (1956).

[2] E. M. Bernstein and H. W. Lewis, Phys. Rev. **105**, 1524 (1957).

[3] T. Huus, J. Bjerregaard, and B. Elbek, Kgl. Danske Videnskab. Selskab, Mat.-fys. Medd. **30**, No. 17 (1956).

[4] M. C. Olesen and B. Elbek, Nuclear Phys. **15**, 134 (1960). See also B. Elbek, K. O. Nielsen, and M. C. Olesen, Phys. Rev. **108**, 406 (1957); V. Ramsak, M. C. Olesen, and B. Elbek, Nuclear Phys. **6**, 451 (1958); B. Elbek, M. C. Olesen, and O. Skilbreid, Nuclear Phys. **10**, 294 (1959).

[5] E. M. Bernstein and H. W. Lewis, Phys. Rev. **100**, 1345 (1955).

[6] E. M. Bernstein, Phys. Rev. **112**, 2026 (1958).

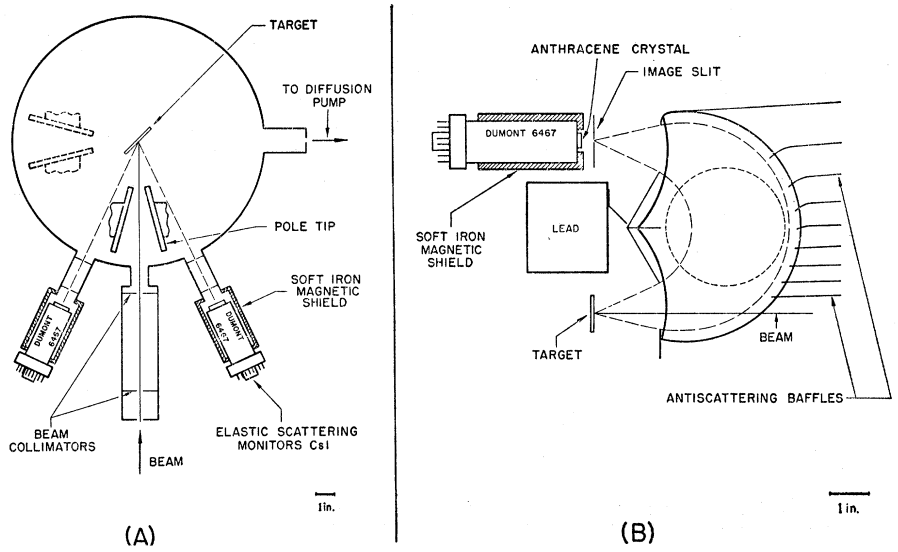

FIG. 1. Schematic of the experimental arrangement. Part (A) is in a horizontal plane containing the beam. The pole tips of the spectrometer are shown in two positions 180° (solid lines) and 90° (dotted lines). Part (B) is in a vertical plane containing the beam. Here the spectrometer is shown at 180° with respect to the beam.

the crossover transition from the second rotational state to the ground state were not observed, in general. Without any information concerning the intensity of the crossover transition it is nevertheless possible to make a self-consistent check of the rotational model.[6]

In order to make a complete, model independent test of the theory using the conversion electron method one must be able to observe most of the conversion lines associated with the decay of the two levels excited. In particular, it is necessary to measure both the K and L conversion lines from the first rotational state transition and the cascade transition, and either the K or the L conversion line from the crossover transition. Due to their low energy it was not possible in the present experimental arrangement to observe all of the lines for Dy^{161}, Dy^{163}, and Tm^{169}. For these nuclei only some of the predictions of the model could be checked.

Detailed discussions of the predictions of the simple rotational model have been given by several authors.[1,3,7] The theoretical predictions which are applicable to the isotopes investigated are given in the tables along with the experimental results.

II. EXPERIMENTAL PROCEDURE

Alpha particles and protons of 2 to 3.7 Mev from the University of Wisconsin electrostatic accelerator (long tank) were used as bombarding particles. The energy of the particles was determined by passing the beam through a 90° electrostatic analyzer which was calibrated to about one part in two thousand with the $Li^7(p,n)$ threshold at 1.881 Mev. The slit system of the analyzer was set to limit the energy spread of the beam to about one part per thousand.

The conversion electron spectra emitted following Coulomb excitation were analyzed by means of a magnetic β-ray spectrometer of the "wedge shaped" design originally developed by Kofoed-Hansen, Lindhard, and Nielsen.[8] After passing through the electrostatic analyzer the ion beam was brought into the vacuum chamber of the spectrometer and struck the target in the normal source position. The beam was collimated by two tantalum diaphragms having apertures 80 mils in diameter and spaced about six inches apart. The arrangement is shown schematically in Fig. 1. Part A of Fig. 1 is in a horizontal plane containing the beam. The spectrometer vacuum chamber is constructed with a sliding O-ring seal so that the spectrometer can be rotated with respect to the beam in order to make angular distribution measurements. The pole tips are shown in two positions, 180° (solid lines) and 90° (dotted lines). For the total cross-section measurements reported here the spectrometer was oriented at 125° with respect to the beam. Since the angular distributions of the conversion electrons are of the form $\omega(\theta)=1+C_2P_2(\theta)+C_4P_4(\theta)$, and for all the cases measured C_4 is less than 0.01, the yield per unit solid angle at 125° (where $P_2=0$) is proportional to the total yield per unit solid angle to better than one percent. In order to limit the angular spread of the electrons accepted by the spectrometer, a circular aperture was placed in front of the gap between the pole tips. This aperture was such that only electrons leaving the target in a cone of half angle of about 12° entered the field region.

The two CsI scintillation counters shown in the figure were used to monitor the bombarding particles elastically scattered from the target. These counters were placed at 155° with respect to the beam, one on each side. At this angle the particles elastically scattered from the rather heavy target nuclei could easily be

[7] M. Martin, P. Marmier, and J. de Boer, Helv. Phys. Acta **31**, 435 (1958).

[8] O. Kofoed-Hansen, J. Lindhard, and O. B. Nielsen, Kgl. Danske Videnskab. Selskab, Mat.-fys. Medd. **25**, No. 16 (1950).

resolved from those scattered from the thick carbon backings. From the elastic scattering rate measured in these counters and the Rutherford scattering relation the target thicknesses were determined to a few percent. Also, since the electron counting rates were measured with respect to the number of elastically scattered particles, the effects of any inhomogeneities in the target were greatly minimized.

Part B of Fig. 1 is in a vertical plane containing the beam. The shape of the spectrometer pole tip is shown along with the position of the target and the image slit. In this view the spectrometer is rotated to the 180° position. A set of baffles was placed in front of the wall of the vacuum chamber opposite the target and image slit to reduce the scattering of particles from this wall into the detector.

The current passing through the magnet coils was used as a measure of the momentum of the electrons which were detected. The magnet current was obtained from an electronic supply and was stabilized to better than one part in two thousand. To reduce the effects of hysteresis, the current was always cycled by increasing it to the maximum value and then decreasing it to zero before each measurement. The reproducibility of the peak position of a given conversion line was, in general, better than one percent. This was considered adequate since the energies of most of the transitions investigated have been determined[9] to a very high degree of precision with a bent crystal gamma-ray spectrometer. For the measurements described here the image slit width and input aperture were such that the momentum resolution was about one percent. The linearity of momentum with magnet current was checked and an absolute calibration was made using the well-known transitions in Cs^{137} and Au^{198} and the 136-kev transition following Coulomb excitation of Ta^{181}.

The electrons were detected with an anthracene scintillation counter. The efficiency of the detector as a function of electron energy was checked by measuring the continuous β spectrum following the decay of Pm^{147} whose Kurie plot is known to be linear[10] down to an energy of $\sim$8 kev. The Kurie plot obtained from the measured spectrum was found to be a straight line within the statistics of a few percent down to an energy of 25 kev where source backing effects began to produce an excess of low-energy electrons. Phototube noise was not appreciable above about 15 kev. Since the lowest energy electrons measured in the present experiment were above 30 kev, it was considered safe to assume a constant detector efficiency over the range of interest. In general, an integral bias was used on the detector. This bias was set to accept the lowest energy which was to be measured in a given spectrum. A differential window was used for some of the weak conversion lines at the higher electron energies, where the background is mainly due to external gamma rays and neutrons produced by the beam hitting slits and the carbon target backings.

The effective solid angle of the spectrometer was determined in the following manner. A source of Cs^{137} was prepared, and the number of K and $L+M$ internal conversion electrons from the 661-kev transition transmitted by the spectrometer per unit time was measured. Then, one of the CsI counters was replaced with the anthracene electron detector, and the electron spectrum emitted by the source was measured directly with the anthracene counter. Although the conversion lines from the various shells were not resolved in the anthracene counter, the resolution was good enough to separate the conversion line peak fairly well from the low-energy continuous β spectrum emitted by Cs^{137}. Since the solid angle intercepted by the detector in this position could be measured readily, the total number of $K+L+M$ conversion electrons emitted into 4π steradians by the source per unit time could be determined. The effective solid angle of the spectrometer is then given by the ratio of the number of $K+L+M$ conversion electrons transmitted per unit time by the spectrometer to the total number of $K+L+M$ electrons emitted by the source per unit time. The value of the solid angle obtained from the measurements was $0.9\pm0.1\%$ of 4π steradian. The uncertainty corresponds to one standard deviation. The value for the effective solid angle is about 20% lower than the geometrical solid angle seen by the input aperture. This indicates some of the electrons are "lost" (in collision with the pole tips, for example) after entering the gap.

The target holder could be moved in the vertical direction so that one of three targets was in the bombarding position. It was found convenient and useful to keep a piece of quartz in one of the target positions to visually check the alignment of the beam. A vacuum interlock was provided so that the target holder could be removed and targets changed without "breaking" the vacuum in the entire chamber.

The thicknesses of the targets used in this type of experiment are extremely important. If the targets are too thick, the low-energy conversion lines are smeared out and self-absorption corrections which are difficult to estimate become large. On the other hand, if the targets are too thin the signal-to-background ratio for the low intensity lines is very small. In some cases it was advantageous and almost necessary to use two targets differing in thickness. The thinner target was used for the low-energy lines, and the thicker one was used for the high-energy lines. Good data could be obtained for the intermediate energy lines from both targets.

The targets were prepared by vacuum evaporation

[9] E. L. Chupp, J. W. M. DuMond, F. J. Gordon, R. C. Jopson, and Hans Mark, Phys. Rev. **112**, 518 (1958).

[10] See, for example, R. O. Lane and D. J. Zaffarano, Phys. Rev. **94**, 960 (1954).

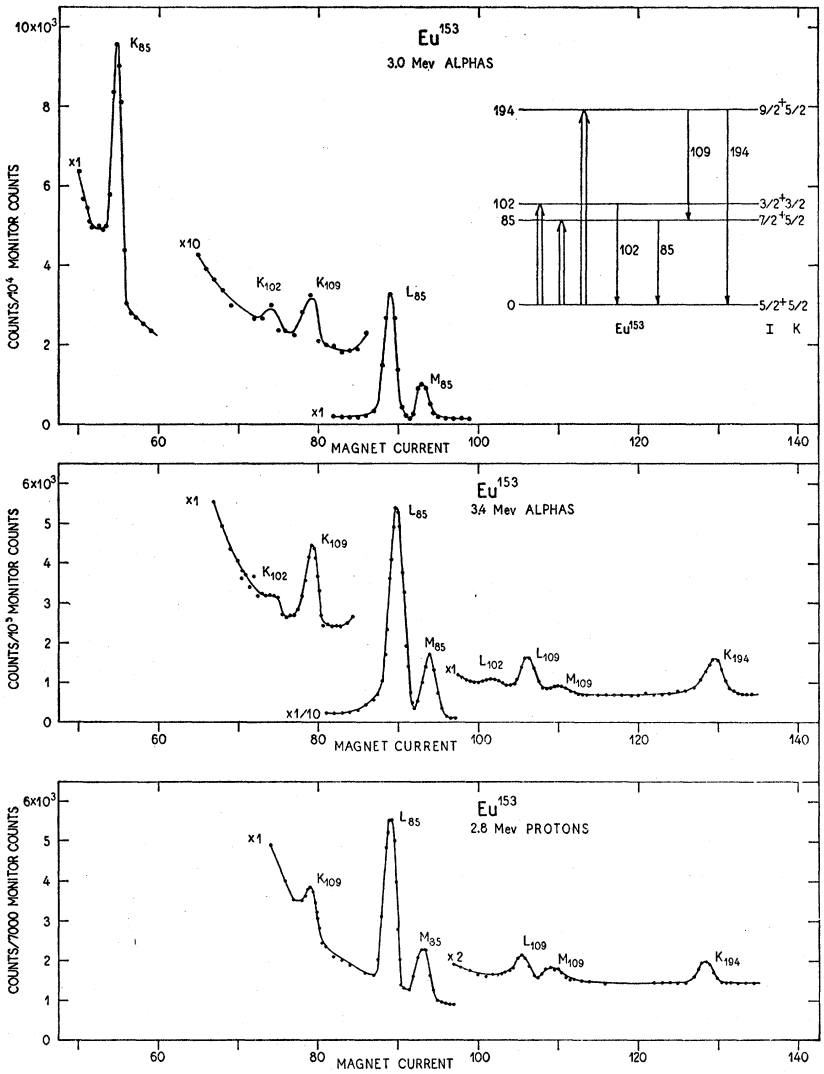

FIG. 2. Internal conversion electron spectra observed following Coulomb excitation of Eu^{153}. The conversion lines are labelled according to the atomic shell and the energy of the transition. Note the several changes of scale.

onto thick carbon backings. The evaporator[11] consisted of a $\frac{1}{4}$-inch diameter, $\frac{1}{4}$-inch long cylindrical carbon post which was heated by electron bombardment. For Ho^{165}, Tm^{169}, Lu^{175}, and Ta^{181} metals were used as the charge material for the evaporator. For Eu^{153}, Dy^{161}, and Dy^{163} oxides enriched in these isotopes at the Oak Ridge National Laboratory were used as the charge material. Because it was difficult to estimate the thicknesses of the targets before they were bombarded, several targets of varying evaporation time were made for each isotope. The thicknesses of the targets to the emerging electrons ranged from about 40 $\mu g/cm^2$ to 400 $\mu g/cm^2$. Since the targets were mounted at an angle of 20° with respect to the beam, the thickness seen by the beam was about three times the thickness seen by the emerging electrons.

Due to the variation of the signal-to-background ratio with bombarding particle and bombarding energy it was found advantageous to measure different parts of the spectrum with different bombarding conditions. The best signal-to-background ratio for the low-energy transitions are obtained with alpha particles, while protons are best for the highest energy transitions. Detailed discussions of the background problems and the bombarding conditions which result in the best signal-to-background ratio for this type of experiment are given in references 1, 2, and 3.

[11] The evaporator was very similar to the one described in reference 4.

III. EXPERIMENTAL RESULTS

Several of the measured conversion electron spectra are shown in Figs. 2 and 3. The background at low electron energies is due to "stopping electrons" from the target and decreases rapidly with increasing electron energy while the rather flat background at the higher electron energies is due mainly to gamma rays and neutrons.

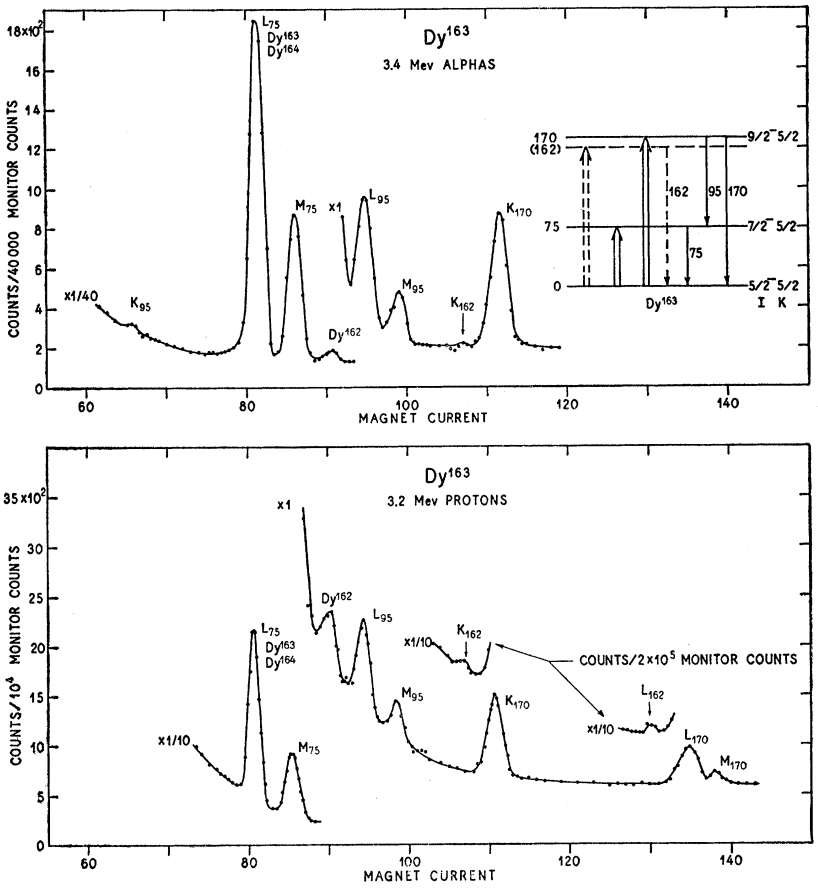

FIG. 3. Internal conversion electron spectra observed following Coulomb excitation of Dy^{163}. Some of the conversion lines are due to the presence of other Dy isotopes in the target. These are labelled according to the isotope. The conversion lines from Dy^{163} are labelled according to the atomic shell and the energy of the transition. Note the several changes of scale. The assignment of the 162-kev transition is tentative (see the text).

All of the transitions observed following Coulomb excitation of the isotopes investigated are listed in Table I along with their assignments. Table II contains the relative intensities of the various conversion lines measured under particular bombarding conditions. The errors quoted correspond to standard deviations. In most cases the errors are on the order of 10% although they depend to a large extent on the intensity of the particular line compared with the background below the line. In general, the statistical uncertainty is small compared to the uncertainty in the background subtraction. An additional uncertainty of a few percent has been added to the assigned error for the lowest energy lines (below about 40 kev) to take care of possible systematic errors due to target thickness effects.

The data for the particular isotopes are discussed in more detail below. In all cases the present results are in reasonable agreement with the earlier conversion electron measurements considering the rather large uncertainties of the latter. Only those cases in which the discrepancies appear to be unusually large will be mentioned.

Eu^{153}

The Eu^{153} targets were enriched to 95% in this isotope; the remaining 5% was Eu^{151}. Measurements of enriched Eu^{151} targets were made also, and the results have been presented in a verbal report.[12] Several of the transitions in the two isotopes have very nearly the same energy and are not resolved; however, since Eu^{151} is not highly deformed, the intensities of the transitions are much lower than the corresponding ones in Eu^{153}. Thus, the subtractions of the contributions of Eu^{151} to the intensities of the conversion lines measured with the Eu^{153} target are much smaller than 5% and do not contribute any uncertainty.

A number of previous measurements[2,3,13] of the conversion electrons following Coulomb excitation of this isotope have been made. The main disagreement with the present results is the K to L ratio for the cascade transition. Reference 2 gives 5.3, reference 13 gives 2.3, and the present value is 3.4 ± 0.25. Part of the discrepancy with the value in reference 2 may be due to angular distribution effects since the measurements reported in reference 2 were made at 90° with respect to the beam.

In addition to the rotational states, the intrinsic

[12] E. M. Bernstein and R. Graetzer, Bull. Am. Phys. Soc. 4, 426 (1959).
[13] C. M. Class and U. Meyer-Berkhout, Nuclear Phys. 3, 656 (1957).

TABLE I. Transitions observed following Coulomb excitation. The assignments are as follows: 1 is the transition from the first rotational state to the ground state, 21 is the cascade from the second to the first rotational state, 2 is the crossover from the second rotational state to the ground state, and "int" denotes a transition involving an intrinsic state.

Isotope	Abundance in target (%)	Target thickness ($\mu g/cm^2$)	Transition energy (kev)	Level energy (kev)	Assignment
Eu^{153}	95	40	85	85	1
		200	109	194	21
			194	194	2
			102	102	int
Dy^{161}	76	200	44	44	1
			58	102	21
			102	102	2
Dy^{163}	74	120	75	75	1
			95	170	21
			170	170	2
			162	(162)	int
Ho^{165}	100	70	95	95	1
		500	115	210	21
			210	210	2
Tm^{169}	100	400	109	118	21
			118	118	2
Lu^{175}	97.4	400	114	114	1
			137	251	21
			251	251	2
			258	750±100	int
Lu^{176}	2.6	400	184	184	1
Ta^{181}	100	40	136	136	1
		500	166	302	21
			302	302	2

state[14] at 102 kev is also excited. The reduced $E2$ transition probability for exciting this level is about 140 times smaller than the probability for exciting the first rotational state at 85 kev. The measured K to L ratio of 3.4 for the 102-kev transition is somewhat lower than the value[14] of about 5 found in β-decay measurements; however, the present determination is rather uncertain.

Dy^{161}

The Dy^{161} target was enriched to 76% in this isotope. Since the energy of the first rotational state is lower than the K-shell binding energy, there is no K conversion for this transition.

Due to the low energy of the cascade transition it was not possible to observe the K conversion line. A value for the $E2$ to $M1$ gamma-ray mixing ratio[15] of $\leqslant 4\%$ $E2$ was obtained for this transition by comparing the partial $B(E2)$ value for L electrons with the total $B(E2)$ value measured in the inelastic scattering experiments.[4]

The K conversion line of the crossover transition was not resolved from the $M+N$ line of the cascade; however, the intensity of the L line of the crossover could be measured fairly well.

The relative intensities of the various conversion lines agree reasonably with a previous measurement.[16] The somewhat higher value for the $E2$ to $M1$ mixing ratio given in the earlier work is due mainly to the fact that different conversion coefficients were used in the analysis of the data. Also, some of the discrepancy is due to the model dependent analysis of the data in reference 16.

Dy^{163}

The Dy^{163} target was enriched to 74% in this isotope. The energy of the first rotational state of Dy^{163} is almost the same as the energy of the first rotational state in Dy^{164} which had an abundance of 18% in the target. Since the $B(E2)$ value for Dy^{164} is larger than the value for Dy^{163} it was necessary to make a rather large subtraction with a resulting increase in the uncertainty of the intensity of this transition. Also, due to the very low energy of the K conversion line for this transition it was not possible to measure its intensity. As in the case of Dy^{161} the $E2$ to $M1$ mixing ratio was obtained by comparing the intensity of the L conversion electrons with the inelastic scattering measurements.[4]

The K line of the cascade (Fig. 3) is very weak as a consequence of the high percentage of $E2$ in this transition. Because of the very low signal-to-background ratio the intensity of this line has a large uncertainty.

In addition to the rotational transitions, a transition of 162 kev is also seen. Evidence for this transition was also seen in the previous conversion electron experiments.[16,17] Angular distribution measurements[18] of the 170-kev gamma rays also indicate the presence of an additional unresolved gamma ray whose angular distribution differs from that expected for the rotational crossover transition.

The relative intensity of the K line of the 162-kev transition and the K line of the 170-kev transition appears to remain constant, within the rather large uncertainty of the former, under different bombarding conditions. This indicates that the 162-kev transition originates from exciting a level whose energy is near 170 kev. For this reason the 162-kev transition is tentatively assigned to a level of that energy. It should be noted that such an assignment is rather arbitrary considering the uncertainties involved. The low K to L ratio of this transition indicates that it is pure $E2$ with possibly a small admixture of $M1$.

[14] D. Strominger, J. M. Hollander, and G. T. Seaborg, Revs. Modern Phys. **30**, 585 (1958).

[15] Throughout this paper the $E2$ to $M1$ mixing ratio and percent $E2$ always refer to the gamma rays and not to the total number of transitions.

[16] E. M. Bernstein and S. Buccino, Bull. Am. Phys. Soc. **3**, 55 (1958).

[17] T. Huus, Proceedings of the Moscow Conference on Nuclear Reactions, 1957 (unpublished), p. 264.

[18] J. de Boer, M. Martin, and P. Marmier, Helv. Phys. Acta **32**, 377 (1959).

The relative intensities of the various conversion lines agree rather well with the previous experiments. The lower $E2$ to $M1$ mixing ratio given in reference 16 is due partly to the model dependent analysis used there, and partly to the fact that the 162-kev and 170-kev K lines were not well resolved in the older measurements and some of the intensity of the 170-kev transition was ascribed to the 162-kev transition.

TABLE II. Relative yields of conversion lines. The rotational transitions are labelled according to the assignments given in Table I. The intrinsic transitions are labelled with the energy and atomic shell. Where two values of the same ratio were measured the individual values are given in column 4 and the weighted average value in column 5.

Isotope	Ratio	Particle and energy (Mev)	Value	Average value
Eu^{153}	K_1/L_1	3.00 α	2.0 ±0.4	2.13 ±0.3
		3.00 α	2.26 ±0.4	
	K_{21}/L_{21}	2.60 p	3.8 ±0.4	
		2.80 p	3.1 ±0.3	
		3.20 α	3.4 ±0.3	3.40 ±0.25
	K_{102}/L_{102}	3.20 α		~3.4
	K_2/L_{21}	2.80 p	0.84 ±0.07	
		3.20 p	0.97 ±0.07	0.92 ±0.05
	K_2/K_{21}	2.80 p		0.27 ±0.02
	K_{21}/L_1	2.60 p		0.24 ±0.03
		2.80 p		0.25 ±0.03
	K_2/L_1	2.60 p		0.059 ±0.006
		2.80 p		0.068 ±0.007
Dy^{161}	L_2/L_{21}	3.00 α		0.14 ±0.016
	L_2/L_1	3.00 α		0.0033±0.0004
	L_{21}/L_1	3.00 α		0.024 ±0.003
Dy^{163}	K_{21}/L_{21}	3.40 α		1.3 ±0.4
	K_2/L_2	3.20 p		2.0 ±0.3
	K_{162}/L_{162}	3.20 p		1.5 ±0.8
	K_2/L_{21}	3.40 α	1.06 ±0.11	
		3.20 p	1.02 ±0.11	1.04 ±0.08
	K_2/L_1	3.20 p		0.066 ±0.008
	L_{21}/L_1	3.20 p		0.065 ±0.008
Ho^{165}	K_1/L_1	3.00 α		6.0 ±0.5
	K_{21}/L_{21}	3.40 α		5.8 ±0.6
	K_2/L_{21}	2.80 p		0.058 ±0.007
	K_{21}/L_1	2.80 p		0.74 ±0.05
	L_{21}/L_1	2.80 p		0.11 ±0.013
		3.20 p		0.13 ±0.013
	K_2/L_1	3.20 p		0.0075±0.0009
Tm^{169}	K_{21}/L_{21}	3.00 α	6.15 ±0.7	
		3.00 α	6.8 ±0.8	6.4 ±0.5
	K_2/K_{21}	3.00 α	0.034±0.004	
		3.00 α	0.030±0.004	0.032 ±0.003
Lu^{175}	K_1/L_1	3.00 α	4.35 ±0.6	
		3.40 α	4.45 ±0.6	4.40 ±0.5
	K_{21}/L_{21}	2.80 p		4.30 ±0.4
	K_2/L_2	3.50 p		2.9 ±0.4
	K_2/L_{21}	3.20 p		0.28 ±0.03
	K_{21}/L_1	2.80 p		0.32 ±0.03
	K_2/L_1	3.20 p		0.24 ±0.03
Lu^{176}	K_1/L_1	3.50 p		~5.2
Ta^{181}	K_1/L_1	3.50 p		4.8 ±0.5
	K_{21}/L_{21}	3.00 p	5.0 ±0.6	
		3.50 p	5.3 ±0.6	5.1 ±0.5
	K_2/L_{21}	3.50 p		0.238 ±0.015
	K_{21}/L_1	3.00 p		0.33 ±0.03
		3.50 p		0.47 ±0.05
	K_2/L_1	3.00 p		0.016 ±0.0014
		3.50 p		0.021 ±0.002

Ho^{165}

Ho^{165} is isotopically pure. All of the conversion lines necessary for a complete check of the model were observed.

Tm^{169}

Tm^{169} is isotopically pure. The first rotational state in Tm^{169} is at 8 kev[14] which is much too low an energy to be seen in the present experiment. Therefore, only measurements of the cascade and crossover transitions from the second rotational state were made.

Lu^{175}

Lu^{175} is 97.4% abundant in natural Lu; the remaining 2.6% is the odd-odd isotope Lu^{176}. The first rotational state transition in Lu^{176} was observed with the natural Lu target and is discussed below.

In addition to the rotational state transitions in Lu^{175}, a relatively strong conversion line at 195 kev was also seen. Due to its high intensity it is extremely unlikely that this line is from Lu^{176}. Since there was no evidence for a K conversion line at the expected energy if the 195-kev line was an L line it is rather certain that it is the K conversion line of a 258-kev transition. The fact that no evidence was found for an L line of the 258-kev transition is to be expected if the multipolarity of the transition is $M1$ or $E1$.

The relative increase of the yield of the 258-kev transition with 3.2- and 3.5-Mev protons indicates that it originates from exciting a level at 750±100 kev.

Assuming that the 258-kev transition is $M1$ and that it occurs as a cascade in all of the de-excitations, one obtains a $B(E2)$ value for exciting a 750-kev level which is about 1/60 of the $B(E2)$ value for exciting the first rotational state at 114 kev. An $E1$ assignment of this transition which is also compatible with its K to L ratio of $\geqslant 5$, would lead to a much larger $B(E2)$ value which would be difficult to understand.

There is, of course, the possibility that the 195-kev conversion line is due to an impurity in the target. However, its rather high intensity and the variation of the yield as a function of energy are not consistent with such an assignment.

A slight indication was also found for the K conversion line of the well-known[14] 229-kev transition in Lu^{175}. The existence of this extremely weak line was not definitely established in the present experiment.

Lu^{176}

Although Lu^{176} is only 2.6% abundant in natural Lu, the K and L conversion lines from the first rotational state at 184 kev were strong enough to be seen. There is no other published information concerning the $E2$ to $M1$ mixing ratio for this transition, but mea-

TABLE III. $E2$ to $M1$ gamma-ray mixing ratios expressed as the $\%E2$. The subscript 1 refers to the first rotational state transition and the subscript 21 refers to the cascade from the second to the first rotational state. Except for the last column which gives the $(\%E2)_{21}$ obtained from gamma-ray angular distribution measurements[a,b] the values are obtained from the K to L ratios given in Table II unless otherwise noted.

Isotope	$(\%E2)_1$	$(\%E2)_{21}$	$\omega(\theta)$[c]
Eu^{153}	40 ± 6	32 ± 4	31 ± 6
Dy^{161}	...	$\leqslant 4$[d]	...
Dy^{163}	80 ± 20[d]	70_{-15}^{+25}	$88_{-6}^{+4.5}$
Ho^{165}	$2.5_{-2.0}^{+3.5}$	5 ± 3	4 ± 2
Tm^{169}	...	$0.6_{-0.6}^{+3}$	2 ± 0.5
Lu^{175}	15 ± 4	17 ± 3	18 ± 2.5
Lu^{176}	15 ± 10	...	...
Ta^{181}	16 ± 1.5[e]	12 ± 8	16 ± 2[f]

[a] See reference 7.
[b] See reference 18.
[c] $(\%E2)_{21}$ obtained from gamma-ray angular distribution measurements.[7,18]
[d] Obtained from the absolute L conversion coefficient.
[e] Average value from the K/L ratio and γ-γ correlation from β decay.[19]
[f] McGowan and Stelson[22] obtained a value of 20 ± 3 which has been averaged with the value of 12 ± 4 given in reference 7.

surements[4] of the inelastically scattered particles have been made using enriched targets. The uncertainty of the electron measurements could be greatly reduced with a target enriched in this isotope.

Ta^{181}

Most of the measurements concerning Ta^{181} are taken from a previous experiment.[6] The additional information obtained in the present work are the absolute $B(E2)$ values and the intensity of the crossover transition which is necessary for the model independent method of analysis presented here.

The values of the $E2$ to $M1$ mixing ratios given here differ slightly from those in reference 6 due to the use of different conversion coefficients in the analysis.

The rather accurate value of $16.5\pm2.5\%$ $E2$ in the first rotational state transition obtained from a gamma-gamma correlation[19] following β decay is in good agreement with the value of $15\pm5\%$ $E2$ obtained here from the K to L ratio. These two values have been averaged to obtain the value of the percent $E2$ given in Table III.

IV. ANALYSIS OF THE DATA

In order to make a comparison of the experimental data with the predictions of the rotational model one must know the absolute $M1$ and $E2$ internal conversion coefficients. There exist two theoretical calculations of K and L shell internal conversion coefficients[20,21] with finite nuclear size and screening effects included. These calculations are in good agreement for the $E2$ coefficients and the $M1$ K-shell coefficients. However, Rose's values for the $M1$ L-shell coefficients are 10 to 15% lower than Sliv and Band's values in the region of atomic number which is of interest. Some of the data were analyzed with both sets of coefficients, and it was found that Sliv and Band's values gave somewhat better agreement between the $M1$ and $E2$ mixing ratios obtained from the K to L ratios and those given in reference 7 which were obtained by gamma-ray angular distribution measurements. For this reason Sliv and Band's values have been used in the analysis presented here. Since the conversion coefficients are large for most cases, many of the results are not very sensitive to the exact value used. Also, for those transitions where there is more than 15% $E2$ the difference between the values obtained with the two sets of coefficients is much less than the quoted experimental uncertainty. The absolute values of the $M1$ to $E2$ mixing ratios obtained from the K to L ratios are affected the most by the different choice of conversion coefficients. However, the ratio of the percent $E2$ in the first rotational state transition to the percent $E2$ in the cascade transition is essentially independent of which coefficients are used.

The $M1$ to $E2$ gamma-ray mixing ratios are obtained from the measured K to L ratios in the usual manner. The results are given in Table III and are expressed as

TABLE IV. Absolute $B(E2)$ values for excitation. The conversion lines are labelled according to the assignments in Table I. ϵ is the fraction of all decays of the particular transition which go by the listed conversion line.

Isotope	Transition	Level energy (kev)	Particle and energy (Mev)	$\epsilon B(E2)/e^2$ 10^{-48} cm^4	$B(E2)/e^2$ 10^{-48} cm^4
Eu^{153}	L_1	85	2.80 p	0.52	2.04 ± 0.4
	L_{21}	194	2.80 p	0.046	
	K_2	194	2.80 p	0.051	0.73 ± 0.14
	K_{102}	102	3.40 α	...	$0.14_{-0.06}^{+0.09}$
Dy^{161}	L_1	44	3.00 α	1.82	2.36 ± 0.6
	L_{21}	102	3.00 α	0.078	
	L_2	102	3.00 α	0.016	0.59 ± 0.14
Dy^{163}	L_1	75	3.20 p	0.8	2.0 ± 0.4
	L_{21}	170	3.20 p	0.052	
	K_2	170	3.20 p	0.055	0.6 ± 0.12
	K_{162}	(162)	3.20 p	...	0.025 ± 0.008
Tm^{169}	L_{21}	118	3.00 p	0.35	
	K_2	118	3.00 p	0.076	3.9 ± 0.7
Ho^{165}	L_1	95	3.20 p	0.328	2.8 ± 0.4
	L_{21}	210	3.20 p	0.055	
	K_2	210	3.20 p	0.0031	0.65 ± 0.13
Lu^{175}	L_1	114	3.20 p	0.358	2.4 ± 0.5
	L_{21}	251	3.20 p	0.044	
	K_2	251	3.20 p	0.012	0.56 ± 0.1
	K_{258}	750	3.50 p	...	0.04 ± 0.006
Ta^{181}	K_1	136	2.60 p	0.99	1.9 ± 0.3
	K_{21}	302	2.60 p	0.14	
	K_2	302	2.60 p	0.007	0.48 ± 0.08

[19] P. Debrunner, E. Heer, W. Kündig, and R. Rüetschi, Helv. Phys. Acta **29**, 745 (1956).
[20] M. E. Rose, *Internal Conversion Coefficients* (North-Holland Publishing Company, Amsterdam, 1958).
[21] L. A. Sliv and I. M. Band, Leningrad Physico-Technical Institute Reports, 1956 [translation: Report 57ICC K1 and Report 58ICC L1, issued by Physics Department, University of Illinois, Urbana, Illinois (unpublished)].

the percent $E2$. Table III also contains the percent $E2$ in the cascade transition which has been determined by angular distribution measurements[7,18,22] of the gamma rays.

While the targets are thin enough so the energy loss for protons of the energy range used is relatively small, the energy loss for alpha particles in this energy range is rather appreciable. In addition, the Coulomb excitation cross section varies more steeply with bombarding energy for alpha particles than for protons. Therefore, in order to eliminate the uncertainties introduced with target thickness corrections, the alpha-particle data were only used to compare the relative intensities of conversion lines which result from excitation of the same level. These are, of course, independent of the effective bombarding energy. Also, except for Dy^{161} where these effects are not important, only the proton data were used to calculate the reduced $E2$ transition

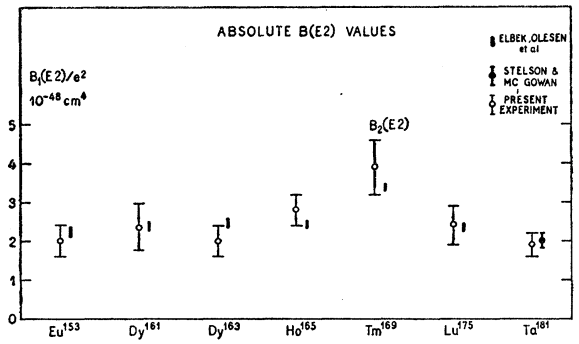

FIG. 4. Absolute $B(E2)$ values for exciting the first rotational state of the isotopes investigated. The value for Tm^{169} is for the second rotational state. The results from this experiment are compared with the much more accurate results from inelastic scattering measurements (reference 4). The length of the points for the inelastic scattering results are the size of the error quoted. For Ta^{181} there have been no inelastic scattering measurements; instead the electron data are compared with rather accurate gamma-ray measurements (reference 22).

probabilities, $B(E2)$.[23] The $B(E2)$ values (Table IV) were calculated from the measured cross sections using the theoretical Coulomb excitation calculations given in reference 1. The errors quoted are standard deviations which include the uncertainties in the measured intensity and the uncertainty in the absolute solid angle of the spectrometer. The $B(E2)$ values for the first rotational state of each isotope (except Tm^{169}) are compared with the very accurate values obtained from the inelastic scattering measurements[4] in Fig. 4.

The other quantities which are of interest are the $E2$ gamma ray branching ratios of the second rotational states $T_{E2}(\gamma_2)/T_{E2}(\gamma_{21})$. The subscript 2 refers to the crossover transition and the subscript 21 refers to the cascade transition. The $E2$ branching ratio can be

[22] F. K. McGowan and P. H. Stelson, Phys. Rev. **99**, 127 (1955), and P. H. Stelson and F. K. McGowan, Phys. Rev. **99**, 112 (1955).

[23] $B(E2)$ is the reduced $E2$ transition probability for excitation and not decay.

TABLE V. Comparison of the experiment with the predictions of the simple rotational model. The values listed under E are the experimental values while those listed under T are the theoretical predictions. B_2/B_1 is the ratio of the reduced transition probability, $B(E2)$, for exciting the second state to the $B(E2)$ value for exciting the first. $T_{E2}(\gamma_2)/T_{E2}(\gamma_{21})$ is the $E2$ gamma-ray branching ratio of the second state. $(\%E2)_1/(\%E2)_{21}$ is the ratio of the $\%E2$ in the first to ground-state transition to the $\%E2$ in the cascade from the second to the first state.

Isotope	B_2/B_1 E	B_2/B_1 T	$T_{E2}(\gamma_2)/T_{E2}(\gamma_{21})$ E	$T_{E2}(\gamma_2)/T_{E2}(\gamma_{21})$ T	$(\%E2)_1/(\%E2)_{21}$ E	$(\%E2)_1/(\%E2)_{21}$ T
Eu^{153}	0.36 ± 0.03	0.350	$6.1\ \pm0.4$	5.86	1.26 ± 0.2	1.03
Dy^{161}	0.25 ± 0.06	0.350	≥ 6	5.86	...	...
Dy^{163}	0.30 ± 0.05	0.350	$6.5\ \pm0.5$	5.86	...	...
Ho^{165}	0.23 ± 0.03	0.257	$2.4_{-0.8}{}^{+1.5}$	4.21	$0.57_{-0.40}{}^{+0.65}$	1.0
Tm^{169}	...	...	4.7 ± 1	4.95	...	...
Lu^{175}	0.23 ± 0.025	0.257	$4.8\ \pm0.65$	4.21	0.86 ± 0.25	1.0
Ta^{181}	0.25 ± 0.025	0.257	4.33 ± 0.55	4.21	$1.0\ \pm0.1$	1.0

expressed in terms of the known conversion coefficients and two experimental measurements which are the percent $E2$ in the cascade transition and the relative intensity of one conversion line from the crossover transition and one from the cascade transition. For example:

$$R\equiv\frac{T_{E2}(\gamma_2)}{T_{E2}(\gamma_{21})}=\frac{K_2}{L_{21}}\frac{1}{\alpha_{K2}}\left[\frac{1-e_{21}}{e_{21}}\beta_{L21}+\alpha_{L21}\right],$$

where α_{K2} is the K-conversion coefficient of the pure $E2$ crossover transition, β_{L21} is the $M1$ L-conversion coefficient of the cascade transition, α_{L21} is the $E2$ L-conversion coefficient of the cascade transition, $e_{21}\times100$ is the percent $E2$ in the cascade transition, and $K2/L21$ is the relative intensity of the K line of the crossover transition and the L line of the cascade transition. With obvious modifications this relation can be written in terms of other experimentally measured intensities such as $K2/K21$, etc. The values of e_{21} used in the calculations were weighted average values of the last two columns in Table III.

V. DISCUSSION

The experimental results and the theoretical predictions of the rotational model are compared in Table V and Figs. 5, 6, and 7. The errors quoted correspond to

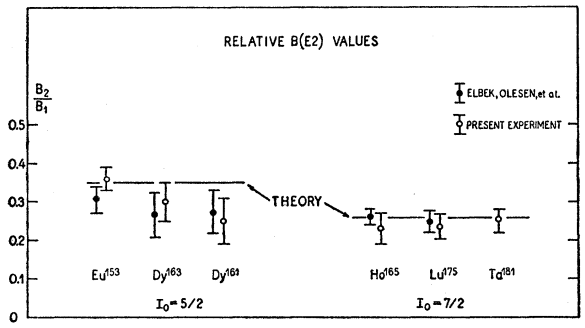

FIG. 5. Relative $B(E2)$ values for exciting the first and second rotational states of the isotopes investigated compared with the predictions of the rotational model and the inelastic scattering data (reference 4).

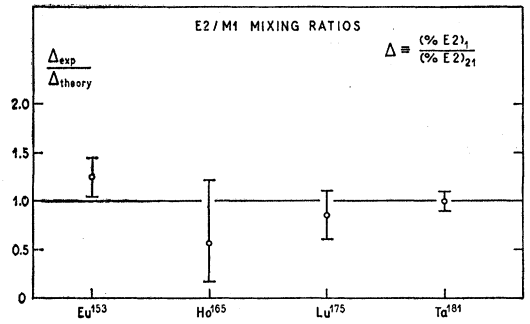

FIG 6. Comparison of the relative $M1$ to $E2$ mixing ratios for the first rotational state transition and the cascade transition with the rotational model.

standard deviations. The magnitudes of the errors vary considerably for different nuclei. The rather large uncertainties for the relative $E2$ to $M1$ mixing ratio and the $E2$ branching ratio of the second rotational state for Ho^{165} are a consequence of the low value of the percent $E2$ for this isotope.

Within the experimental uncertainties there is general agreement between the theoretical predictions and the measured values. However, the ratios of $B_2(E2)/B_1(E2)$ for the Dy isotopes are somewhat lower than the theory. This is in agreement with the inelastic scattering results. Averaging the electron data with the inelastic scattering data one obtains B_2/B_1 values of 0.26 ± 0.04 and 0.28 ± 0.04 for Dy^{161} and Dy^{163}, respectively. These average values are about two standard deviations below the theoretical prediction of 0.35.

The basic assumption of the simple rotational model is that the collective rotational motion of highly deformed nuclei is slow enough so that the rotations do not disturb the intrinsic configurations of the individual particles in the nucleus. Since in odd-A nuclei the spacing of the intrinsic states corresponding to single-particle excitations is often of the same magnitude as the rotational excitations, one would expect the above assumption to break down to a certain extent. The consequent coupling between the rotational and intrinsic motions would modify the rotational state transition probabilities somewhat from those predicted for pure rotational motion. Theoretical estimates of the magnitude of the perturbations of the rotational transition probabilities caused by this coupling indicate a rather small ($<10\%$) correction even for strong coupling. Thus, the deviation of the values for the Dy isotopes seem to be somewhat larger than expected from this type of perturbation.

If the coupling between the intrinsic and rotational motion is reasonably strong, one should be able to observe transitions resulting from Coulomb excitation of the intrinsic states which are coupled to the ground-state rotational band.[24] The rather large $B(E2)$ values (compared with single-particle estimates) observed for the nonrotational transitions in Eu^{153}, Dy^{163}, and Lu^{175} are probably due to this effect.

ACKNOWLEDGMENTS

Many people in the low-energy nuclear physics group at the University of Wisconsin contributed to the success of this experiment through valuable discussions and suggestions. The authors would especially like to express their gratitude to Professor H. T. Richards for his continuing interest in this work and for many helpful discussions concerning experimental techniques. Thanks are also due to A. Swenson and P. Schultz of the physics department instrument shop for constructing the spectrometer and vacuum chamber, to

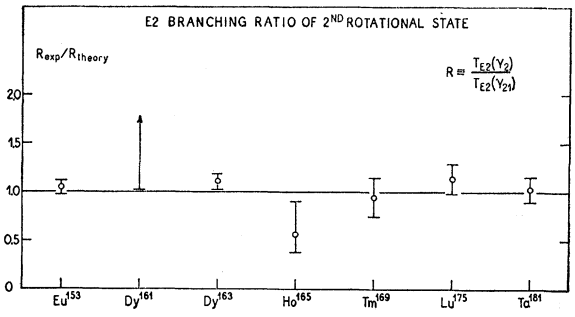

FIG. 7. Comparison of the $E2$ gamma-ray branching ratios of the second rotational state with the rotational model. For Dy^{161} only a lower limit could be obtained from the available data.

M. Murray who designed the magnet current control circuit and kept the electronic equipment working, and to Mr. C. Vought who was extremely helpful in keeping the accelerator running.

One of us (E. M. B.) would like to acknowledge a grant from the National Science Foundation which was in effect during the time the data were being analyzed, and to express his appreciation to Professor Niels Bohr and the staff of the Institute for Theoretical Physics in Copenhagen for the excellent working conditions provided by them. Several discussions with Professor Aage Bohr and Professor B. R. Mottelson and Dr. P. Chr. Hemmer, Dr. T. Huus, and Dr. J. de Boer, which were very much appreciated, were helpful in the interpretation of the data.

[24] A. Kerman, Kgl. Danske Videnskal. Selskab, Mat.-fys. Medd. **30**, No. 15 (1955).